Supporting Information

Sun *et al.* 10.1073/pnas.0710793105

SI Text

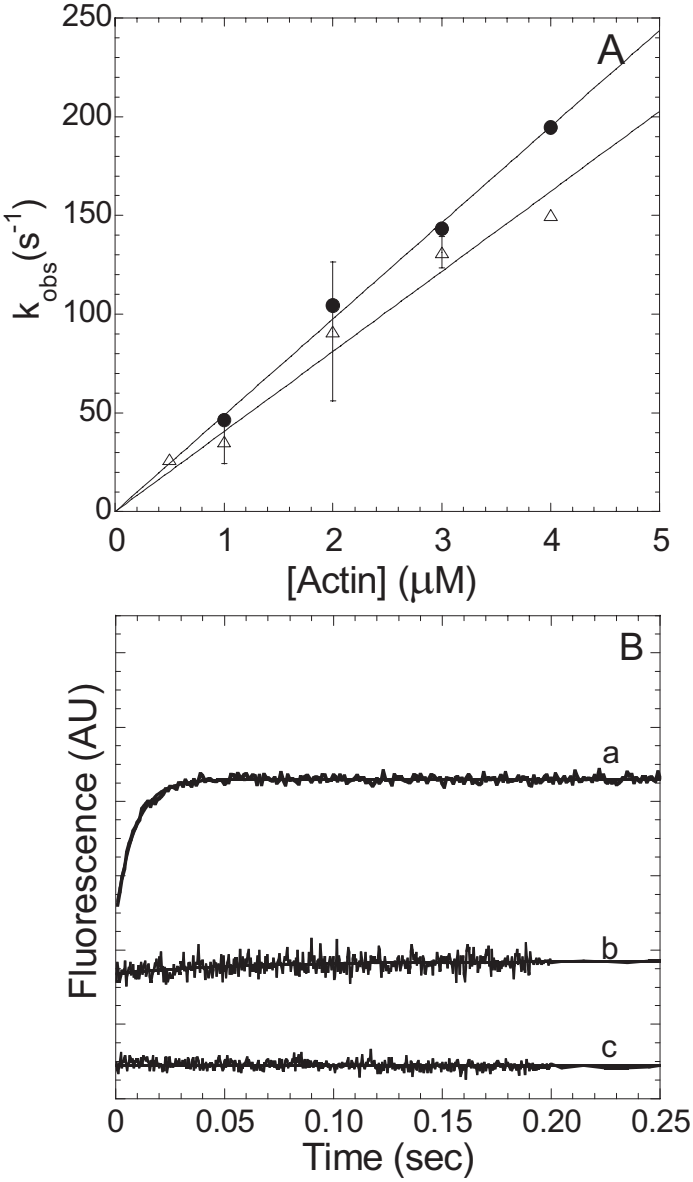

Fig. S1. Kinetics of MV FlAsH binding to I-actin or pyrene actin in the rigor state. (*A*) The rate of the FlAsH or pyrene fluorescence change (k_{obs}) on binding of 0.4 μM or 0.8 μM MV FlAsH to increasing concentrations of I-actin (open triangles) or pyrene actin (filled circles for rigor state) was monitored in the stopped flow. The second-order binding constants were determined from the linear fit of the data. (*B*) Sample traces of the FRET signal from 0.4 μM MV FlAsH binding to 2 μM I-actin (*a*), as well as the donor-only (*b*) and acceptor-only (*c*) controls. The fluorescence transient due to FRET (*a*) was fit to a single-exponential, k_{obs} = 115 $\pm$ 3.0 s^{-1}.

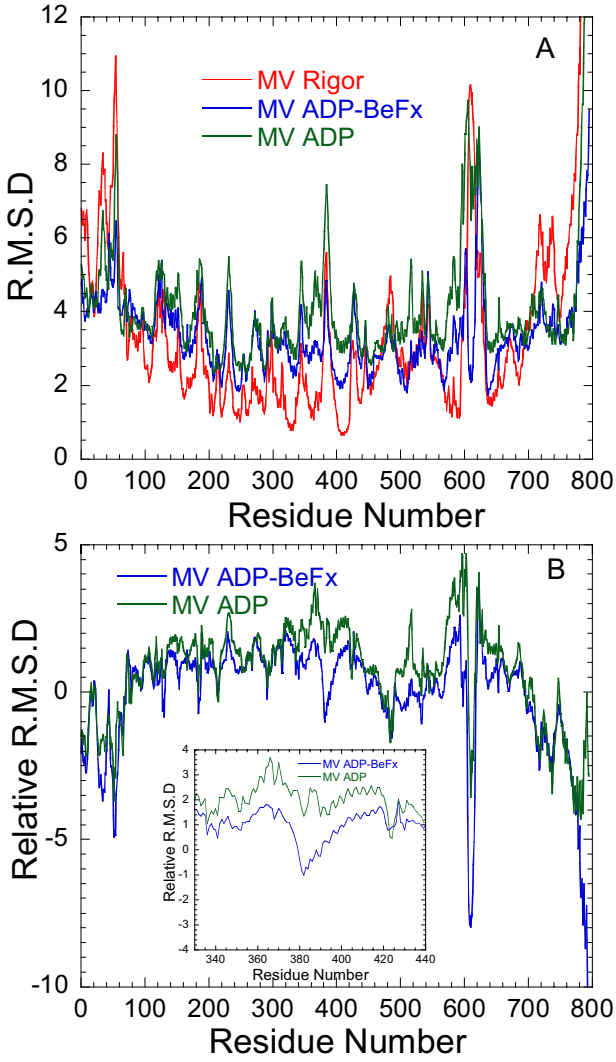

Fig. S2. Mobility in the MV structures studied with an all atom geometric simulation. FIRST (1) was used to determine the number of independent degrees of freedom and identify flexible and rigid regions within each structure. A FIRST analysis depends on a user-selected hydrogen bond energy cutoff parameter. Hydrogen bonds with energy less than the cutoff are modeled as a mechanical constraint. Rigid regions are determined based on covalent bond constraints, hydrophobic constraints, and hydrogen bond constraints. The energy cutoff parameter was adjusted to make a series of structures ranging from being very rigid to very flexible. The total number of independent degrees of freedom ranged from 200 to 1,200, incrementing by 200. FRODA (2) is a geometric simulation based on FIRST output where atomic pair distances within rigid regions are fixed. Monte Carlo moves biased by Ramachandran preferences are applied in flexible regions, and a minimalistic energy function prevents atomic clashing. Each of the six FIRST outputs with a different number of independent degrees of freedom within each structure was simulated for 500,000 successful Monte Carlo moves. Having (less, more) independent degrees of freedom roughly corresponds to (low, high) temperature. The root-mean-square displacement (rmsd) for carbon-alpha atoms was calculated for all cases, where no qualitative differences were found. Statistical errors were minimized for each structure by taking the average over all six cases per structure. (*A*) Root-mean-square displacement (rmsd) is calculated for myosin V Rigor (red), ADP-BeF_X (blue), and ADP (green) conformational states. Higher rmsd signifies alpha carbons having increased motion in three dimensions from their mean positions. (*B*) The rmsd values of myosin V ADP-BeF_X (blue) and ADP (green) relative to the Rigor conformational state. Deviation from zero implies an increased or decreased mobility of the alpha carbon atoms on addition of nucleotide. (*Inset*) Region (residues 330–440) of the upper-50-kDa domain that is more rigid in the ADP-BeF_X state than Rigor and ADP. Three x-ray crystal structures from the Protein Data Bank (PDB ID codes 1OE9, 1W7J, and 1W7I) were, respectively, used to represent the Rigor, ADP-BeF_X, and ADP conformational states of myosin V. All structures were missing residues within loop 2 that minimally span residues 595–631. The MOE software by Chemical Computing Group was used to place all missing residues and missing heavy atoms into the structures. Furthermore, Loop 2 was reconstructed by using the homology modeling function and hydrogen atoms were added assuming a pH of 7. Finally, the energy of each structure was minimized.

1. Jacobs DJ, Rader A, Kuhn LA, Thorpe MF (2001) Protein flexibility predictions using graph theory. *Proteins* 44:150–165.
2. Wells S, Menor S, Hespenheide B, Thorpe MF (2005) Constrained geometric simulation of diffusive motion in proteins. *Phys Biol* 2:S127–S136.

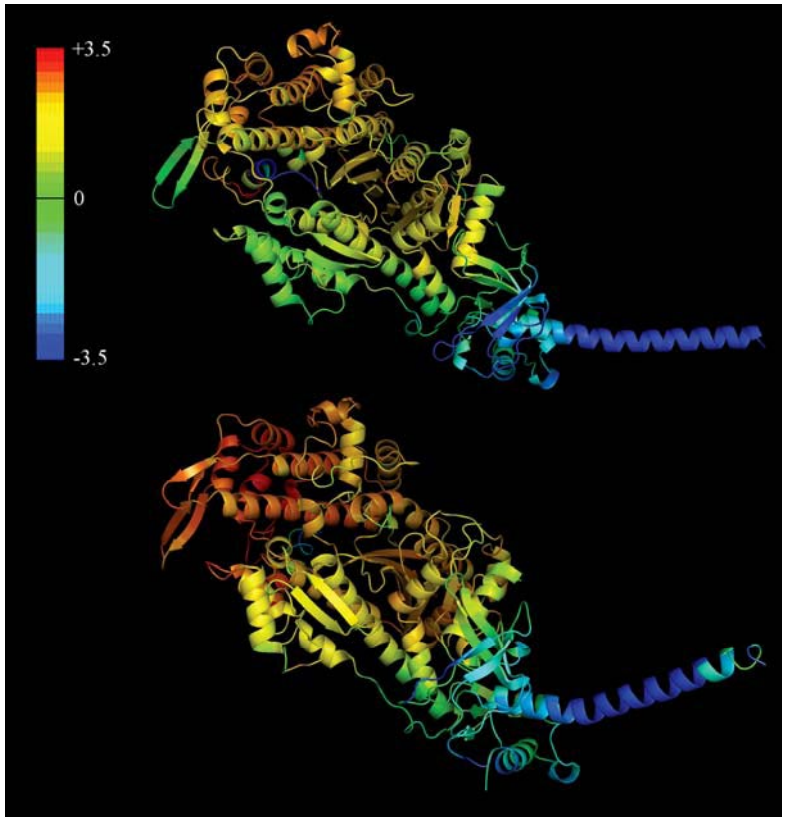

Fig. S3. Ribbon renderings for the relative rmsd in the ADP-BeF_X (*Top*) and ADP (*Bottom*) crystal structures with respect to the rigor state. Blue and red indicates a relative rmsd of −3.5 Å and + 3.5 Å, respectively, where the color spectrum is uniformly distributed with green representing no change in mobility from the rigor conformation.

Table S1. Summary of I-actin fluorescence lifetime data from one dataset of E442A MV FlAsH complexed with I-actin in the presence and absence of ATP

MV:I-actin complex	τ (unbound)	α (unbound)	τ_1, ns	α_1	τ_2, ns	α_2	$\langle\tau\rangle$, ns
E442A MV (Rigor)*	NA	NA	15.35 ± 0.09	0.63	0.92 ± 0.18	0.37	10.07 ± 1.97
E442A MV FlAsH (Rigor)*	NA	NA	9.26 ± 0.08	0.43	2.76 ± 0.09	0.57	5.6 ± 0.18
E442A MV (ATP)†	17.48 ± 0.33	0.31	16.23 ± 0.37	0.27	1.58 ± 0.16	0.41	10.49 ± 1.11
E442A MV FlAsH (ATP)†	17.82 ± 0.07	0.27	11.18 ± 0.10	0.19	1.04 ± 0.10	0.54	7.49 ± 0.72

*The I-actin fluorescence lifetime decays were fit to a two-exponential function for the rigor complexes (0.5 μM I-actin and1.0 μM MV or MV FlAsH).
†The I-actin fluorescence lifetime decays were fit to a three-exponential function in the presence of 1 mM ATP (0.5 μM I-actin and 2.8 μM MV or MV FlAsH), to separate the bound and unbound components. The lifetime of the unbound component was similar to that of I-actin alone (data not shown).

Table S2. Anisotropy measurements of the donor and acceptor fluorophores

Nucleotide states	r_0*	r†
I-actin: E442A MV (rigor)‡	0.280 ± 0.016	0.191 ± 0.012
I-actin: E442A MV (ATP)§	0.276 ± 0.016	0.184 ± 0.011
Actin: E442A MV FlAsH (rigor)‡	0.338 ± 0.006	0.305 ± 0.006
Actin: E442A MV FlAsH (ATP)§	0.369 ± 0.005	0.343 ± 0.007

*The limiting anisotropy measured for the IAEDANS probe (ATP and rigor conditions as described above in KMg50 buffer containing 55% glycerol) and for the FlAsH probe (ATP and rigor conditions as described above in KMg50 buffer containing 33% glycerol) at −14°C.

†The steady-state anisotropy measured as described above for ATP and rigor in KMg50 buffer at 25°C.

‡The IAEDANS probe (0.5 μM I-actin and 1.0 μM E442A MV) and the FlAsH probe (1.0 μM actin and 0.5 μM MV FlAsH) were measured in the rigor state.

§The IAEDANS probe (0.5 μM I-actin and 2.5 μM E442A MV) and the FlAsH probe (2.5 μM actin and 0.5 μM MV FlAsH) were measured in the presence of 1 mM ATP.